

This discussion paper is/has been under review for the journal Biogeosciences (BG).
Please refer to the corresponding final paper in BG if available.

Changes in soil organic carbon storage predicted by Earth system models during the 21st century

K. E. O. Todd-Brown¹, J. T. Randerson¹, F. Hopkins¹, V. Arora², T. Hajima³,
C. Jones⁴, E. Shevliakova⁵, J. Tjiputra⁶, E. Volodin⁷, T. Wu⁸, Q. Zhang⁹, and
S. D. Allison^{10,1}

¹Department of Earth System Science, University of California, Irvine, California, USA

²Canadian Centre for Climate Modelling and Analysis, Environment Canada, University of Victoria, Victoria, British Columbia, Canada

³Japan Agency for Marine–Earth Science and Technology, Yokohama, Japan

⁴Met Office Hadley Centre, Exeter, UK

⁵Department of Ecology and Evolutionary Biology, Princeton University, Princeton, New Jersey, USA

⁶Uni Klima, Uni Research, Bergen, Norway

⁷Institute of Numerical Mathematics, Russian Academy of Sciences, Moscow, Russia

⁸Beijing Climate Center, China Meteorological Administration, Beijing, China

⁹College for Global Change and Earth System Science, Beijing Normal University, Beijing, China

BGD

10, 18969–19004, 2013

Soil carbon changes
in Earth system
models

K. E. O. Todd-Brown et al.

[Title Page](#)

[Abstract](#)

[Introduction](#)

[Conclusions](#)

[References](#)

[Tables](#)

[Figures](#)

[◀](#)

[▶](#)

[◀](#)

[▶](#)

[Back](#)

[Close](#)

[Full Screen / Esc](#)

[Printer-friendly Version](#)

[Interactive Discussion](#)



¹⁰Ecology and Evolutionary Biology Department, University of California, Irvine, California, USA

Received: 11 November 2013 – Accepted: 23 November 2013 – Published: 4 December 2013

Correspondence to: K. E. O. Todd-Brown (ktoddbro@uci.edu)

Published by Copernicus Publications on behalf of the European Geosciences Union.

BGD

10, 18969–19004, 2013

Soil carbon changes in Earth system models

K. E. O. Todd-Brown et al.

[Title Page](#)

[Abstract](#)

[Introduction](#)

[Conclusions](#)

[References](#)

[Tables](#)

[Figures](#)

◀

▶

[Back](#)

[Close](#)

[Full Screen / Esc](#)

[Printer-friendly Version](#)

[Interactive Discussion](#)



Abstract

Soil is currently thought to be a sink for carbon; however, the response of this sink to increasing levels of atmospheric carbon dioxide and climate change is uncertain. In this study, we analyzed soil organic carbon (SOC) changes from 11 Earth system models (ESMs) under the historical and high radiative forcing (RCP 8.5) scenarios between 1850 and 2100. We used a reduced complexity model based on temperature and moisture sensitivities to analyze the drivers of SOC losses. ESM estimates of SOC change over the 21st century (2090–2099 minus 1997–2006) ranged from a loss of 72 Pg C to a gain 253 Pg C with a multi-model mean gain of 63 Pg C. All ESMs showed cumulative increases in both NPP (15 % to 59 %) and decreases in SOC turnover times (15 % to 28 %) over the 21st century. Most of the model-to-model variation in SOC change was explained by initial SOC stocks combined with the relative changes in soil inputs and decomposition rates ($R^2 = 0.88, p < 0.01$). Between models, increases in decomposition rate were well explained by a combination of initial decomposition rate, ESM-specific Q_{10} -factors, and changes in soil temperature ($R^2 = 0.80, p < 0.01$). All SOC changes depended on sustained increases in NPP with global change (primarily driven by increasing CO_2) and conversion of additional plant inputs into SOC. Most ESMs omit potential constraints on SOC storage, such as priming effects, nutrient availability, mineral surface stabilization and aggregate formation. Future models that represent these constraints are likely to estimate smaller increases in SOC storage during the 21st century.

1 Introduction

The global pool of soil organic carbon (SOC) is large relative to atmospheric CO_2 (Jobbagy and Jackson, 2000) and changes in soil–atmosphere fluxes of carbon have the potential to provide either a positive or negative feedback to climate over the next century. The contemporary soil carbon sink in forests is estimated to be approximately

BGD

10, 18969–19004, 2013

Soil carbon changes in Earth system models

K. E. O. Todd-Brown et al.

[Title Page](#)

[Abstract](#)

[Introduction](#)

[Conclusions](#)

[References](#)

[Tables](#)

[Figures](#)

◀

▶

◀

▶

[Back](#)

[Close](#)

[Full Screen / Esc](#)

[Printer-friendly Version](#)

[Interactive Discussion](#)



0.9 PgCyr⁻¹ (Pan et al., 2011). However, uncertainties in the response of soil inputs and heterotrophic respiration to various global change drivers, along with difficulties in measuring heterogeneous SOC pools, lead to relatively large uncertainties in below-ground flux estimates (Houghton, 2003; Le Quéré et al., 2009). The balance of SOC over the next century is even more uncertain (Friedlingstein et al., 2006). Much of this uncertainty is due to the environmental sensitivities of SOC input and output fluxes which depend on environmental variables that will likely change with climate over the next century (Giorgi, 2006).

Net primary production (NPP) provides the primary input of carbon to soil and is sensitive to climate. NPP generally increases with temperature, moisture, and CO₂ up to some functional maximum, in turn providing increased carbon inputs to soil (Chapin and Eviner, 2007; Körner, 2006). Free-air CO₂ enrichment (FACE) studies have shown that NPP increases by 23 % on average across forest ecosystems in response to CO₂ increases from 365 to 550–580 ppm (Norby et al., 2005). However, increases in NPP may be constrained by available nutrients; the theory of progressive nutrient limitation posits that NPP responses to elevated CO₂ will be limited by the supply of soil nutrients, particularly nitrogen (Luo et al., 2004; Norby and Zak, 2011; Nowak et al., 2004). Results from one FACE site support this theory; at the Oak Ridge FACE experiment, NPP increase declined from 23 % to 9 % between years 6 and 11 due to nitrogen limitation (Norby et al., 2010).

In addition, it is not clear whether increases in NPP will translate into increased SOC storage. FACE studies often observe no change in SOC despite increased NPP, although this may be due to the short timescale of the experiments relative to soil turnover times and spatial heterogeneity in SOC pools (Schlesinger and Lichter, 2001). Mechanisms such as priming may also counteract increases in SOC inputs and may explain the lack of SOC accumulation in FACE studies. With priming, fresh carbon inputs associated with increasing NPP stimulate the microbial decomposition of SOC (Fontaine et al., 2004; Kuzyakov et al., 2000).

BGD

10, 18969–19004, 2013

Soil carbon changes in Earth system models

K. E. O. Todd-Brown et al.

[Title Page](#)

[Abstract](#)

[Introduction](#)

[Conclusions](#)

[References](#)

[Tables](#)

[Figures](#)

[|◀](#)

[▶|](#)

[◀](#)

[▶](#)

[Close](#)

[Full Screen / Esc](#)

[Printer-friendly Version](#)

[Interactive Discussion](#)



Heterotrophic respiration is the primary loss pathway for SOC and is also sensitive to climate change. Heterotrophic respiration generally increases with temperature (Davidson and Janssens, 2006) and moisture levels in well drained soils (Cook and Orchard, 2008) but is not directly sensitive to atmospheric CO₂ concentrations. Many 5 studies have hypothesized that rising temperatures will increase SOC losses through decreased soil turnover times (Davidson and Janssens, 2006; Lloyd and Taylor, 1994). Such changes should increase heterotrophic respiration, especially in the high northern latitudes (Schuur et al., 2008), and contribute to increases in global atmospheric CO₂ (Koven et al., 2011). However, other effects like aggregate formation and mineral- 10 organic interactions could stabilize SOC on long time scales, limiting the response to increased temperature (Dungait et al., 2012; Six et al., 2002; Torn et al., 1997).

Earth system models (ESMs) are the primary tools for predicting climate impacts on SOC storage at the global scale. Previous studies have shown that within and between ESMs, variations in contemporary SOC stocks were mostly driven by model estimates 15 of NPP, parameterizations of the intrinsic decomposition rate (fitted at 15 °C and optimal soil moisture), and the temperature sensitivity of heterotrophic respiration (Todd-Brown et al., 2013). Because of the potential importance of SOC for future carbon–climate feedbacks, the goal of our current study was to evaluate ESM estimates of global SOC changes during the 21st century from ESM estimations in the fifth phase of the Coupled 20 Model Intercomparison Project (CMIP5). Specifically, we aimed to (1) compare SOC changes over the 21st century across ESMs, (2) identify the drivers of SOC change within and between ESMs, and (3) assess the reliability of ESM projections by evaluating these drivers and SOC changes in the context of global datasets and empirical findings available from global change studies.

BGD

10, 18969–19004, 2013

Soil carbon changes in Earth system models

K. E. O. Todd-Brown et al.

Title Page	
Abstract	Introduction
Conclusions	References
Tables	Figures
◀	▶
◀	▶
Back	Close
Full Screen / Esc	
Printer-friendly Version	
Interactive Discussion	

2 Methods

2.1 Earth system models

Outputs from Earth system models (ESMs) that contributed to the CMIP5 (Taylor et al., 2011) were downloaded from the Earth System Grid Federation repository. The terrestrial decomposition sub-models of these ESMs all use systems of first-order linear ordinary differential equations with 1–9 substrate pools. The decomposition and transfer rates of the substrate pools have temperature sensitivities that are either: Q_{10} , Arrhenius, increase to an optimal point and then decrease, or some linear approximation of these functions. In response to soil moisture, decomposition rates either increase 5 monotonically or increase to an optimal point and then decrease (Table S1, extended from Todd-Brown et al., 2013).

Model outputs from the historical and RCP 8.5 experiments (Taylor et al., 2011) were downloaded from the CMIP5 repository. The historical simulations were forced with observation-based estimates of CO_2 and other greenhouse gas mixing ratios, aerosol 15 emissions, and land use change scenarios, where appropriate, from 1850–2005. Some models also incorporated natural variability through specified changes in solar radiation and volcanic activity. All models started at 1850 except for GFDL-ESM2G and HadGEM2-ES, which began at 1861 and 1860, respectively. The RCP 8.5 is a high radiative forcing “business as usual” future scenario with a prescribed atmospheric CO_2 20 mole fraction ranging from 378 to 935 ppm for the period 2006–2100. The outputs from the historical and RCP 8.5 experiments were merged to create a continuous record from 1850 to 2100 (Table S1). We chose to use model runs with prescribed CO_2 concentrations, as opposed to emissions-driven experiments, for consistent comparison 25 of the strength of the CO_2 fertilization effects across models and to avoid changes in projected temperature and climate variability due to different CO_2 concentrations in the models.

We used monthly globally-gridded SOC, litter, coarse woody debris carbon, soil temperature, total soil water, heterotrophic respiration, and NPP in our analysis (cSoil,

BGD

10, 18969–19004, 2013

Soil carbon changes in Earth system models

K. E. O. Todd-Brown et al.

Title Page	
Abstract	Introduction
Conclusions	References
Tables	Figures
◀	▶
◀	▶
Back	Close
Full Screen / Esc	
Printer-friendly Version	
Interactive Discussion	



cLitter, cCwd, tsl, mrs0, rh, and npp respectively from the CMIP5 variable list). The reported monthly values for each model were averaged to create annual gridded means. Not all ESMs reported litter or coarse woody debris carbon; thus soil, litter, and coarse woody debris carbon variables were summed and are referred to as “soil organic carbon” (SOC) throughout this analysis. If multiple ensembles were reported for an individual model then the ensembles were averaged. Global totals and means were constructed using the land cell area and the land surface fraction (areacella and sftlf respectively). Soil temperature used in this analysis was calculated from the weighted average from the top 10 cm. Soil water was expressed as a gridded fractional soil water content calculated from the total soil water content divided by the maximal soil water content in the first 10 yr of the historical run. In general, ESMs did not maintain soil carbon balance with the carbon flux variables described above (additional carbon fluxes that consume or diverted NPP in some ESMs included grazing, harvest, land use change, and fire); thus we computed annual soil inputs for each model as the annual change in SOC (ΔC) plus the carbon lost due to heterotrophic respiration (R) summed for each year, i.e. $I = \Delta C + R$. Soil turnover times (inverse of the decomposition rates) were calculated annually from gridded and global totals of SOC stocks and heterotrophic respiration. Soil carbon sinks were calculated from the gridded and global annual differences in SOC stocks.

Many modeling centers submitted multiple ESMs to the repository. In these cases, one model was selected from each model center for analysis. If a model was recommended by the modeling center, that model was used. Otherwise, the model with the highest grid resolution was used. Finally, if no model was preferred by the modeling center and the models were of equal resolution, then a model was randomly selected.

We selected one ESM per modeling center because there were high correlations in the spatial distribution of 21st century SOC change across models from a given modeling center. In general, estimates of SOC changes in models from the same center were more similar than estimates from different modeling centers (Fig. S1), similar to previous results with modern SOC distributions (Todd-Brown et al., 2013). Thus model

BGD

10, 18969–19004, 2013

Soil carbon changes in Earth system models

K. E. O. Todd-Brown et al.

[Title Page](#)

[Abstract](#)

[Introduction](#)

[Conclusions](#)

[References](#)

[Tables](#)

[Figures](#)

◀

▶

◀

▶

[Back](#)

[Close](#)

[Full Screen / Esc](#)

[Printer-friendly Version](#)

[Interactive Discussion](#)



outputs from the same center are non-independent, which could inflate the significance of statistical tests (e.g., regressions) applied to multiple models. In some cases, models from different centers also produced highly correlated predictions because they used the same land carbon sub-model (e.g., CCSM4, CESM1, and NorESM1). In these 5 cases, we still included one model from each center so as not to exclude other factors that might differ across modeling centers, including ocean and atmospheric components of the ESMs that influence precipitation and land surface temperatures. We emphasize that these model predictions are not completely independent and that statistical tests based on them should be interpreted with caution.

10 2.2 Biome definitions

We conducted biome-level analyses by constructing a common biome mask (similar to Todd-Brown et al., 2013). We downloaded vegetation type classifications for 2001–2009 from the MODIS satellite mission to construct the biome map (Friedl et al., 2010; NASA Land Processes Distributed Active Archive Center (LP DAAC), 2008). The vegetative area coverage was regridded from the 0.05×0.05 MODIS grid to each individual 15 ESM grid cell using an area-weighted scheme. The maximal vegetation type for an individual grid cell was then used to assign a biome.

2.3 Contribution of inputs and outputs to SOC change

We used two techniques to separate the relative contributions of changes in carbon 20 inputs and outputs to the total change in SOC over time. For the first technique, we constructed two possible temporal scenarios for gridded SOC stock evolution to illustrate the relative impact of changes in inputs vs. decomposition rate on SOC. In the “constant decomposition rate” scenario, soil carbon inputs evolved as predicted by the model but the SOC decomposition rate was held constant at the 1850 value. In the 25 “constant soil inputs” scenario, decomposition rate evolved as predicted by the model but soil carbon input was held constant at the 1850 value.

BGD

10, 18969–19004, 2013

Soil carbon changes in Earth system models

K. E. O. Todd-Brown et al.

Title Page	
Abstract	Introduction
Conclusions	References
Tables	Figures
◀	▶
◀	▶
Back	Close
Full Screen / Esc	
Printer-friendly Version	
Interactive Discussion	



For the second technique, we modeled ESM change in soil carbon as a function of the change in soil inputs and decomposition rate. First we assumed that the change in soil carbon is equivalent to the change in steady state soil carbon (soil inputs equal to soil outputs) from the start to the end of the 21st century:

$$5 \quad C_{\text{end}} - C_{\text{start}} = \frac{I_{\text{end}}}{k_{\text{end}}} - \frac{I_{\text{start}}}{k_{\text{start}}} \quad (1)$$

where C_{end} and C_{start} are averaged over 2090–2099 and 1997–2006 respectively; C is the global soil carbon stock; I is the associated average soil carbon input; and k is the decomposition rate calculated from global heterotrophic respiration and soil carbon stocks. We can rearrange this equation and correct for the deviation from steady state at the starting time period to generate the following:

$$10 \quad C_{\text{end}} - C_{\text{start}} = \left(\frac{I_{\text{end}} \times k_{\text{start}}}{I_{\text{start}} \times k_{\text{end}}} - 1 \right) C_{\text{start}} \quad (2)$$

15 Using regression analysis with the terms on the right-hand side of Eq. (2), we assessed the relative contributions of changes in soil inputs, changes in decomposition rate, and initial soil carbon stocks to changes in ESM soil carbon.

2.4 Drivers of changes in heterotrophic respiration and decomposition rate

To investigate the drivers of heterotrophic respiration change and decomposition, we used a reduced complexity model (Todd-Brown et al., 2013). This model first assumed 20 that the change in heterotrophic respiration is proportional to total SOC:

$$R = kC \quad (3)$$

25 where R is the heterotrophic respiration, k is the decomposition rate (inverse of the turnover time), and C is the total SOC. We then evaluated drivers of the change in decomposition rate (k) by assuming decomposition rate is dependent on the intrinsic

[Title Page](#)

[Abstract](#)

[Introduction](#)

[Conclusions](#)

[References](#)

[Tables](#)

[Figures](#)

◀

▶

◀

▶

[Back](#)

[Close](#)

[Full Screen / Esc](#)

[Printer-friendly Version](#)

[Interactive Discussion](#)



decomposition rate (k_0 , spatially and temporally constant) times the temperature sensitivity of decomposition ($Q_{10}(T)$) and soil moisture sensitivity (W raised to the power b) for each model:

$$k = k_0 Q_{10}^{(T-15/10)} W^b \quad (4)$$

where the temperature (T) sensitivity function represents a Q_{10} -factor increase for each 10 °C of warming from a 15 °C baseline, and the moisture sensitivity function is monotonically increasing (b greater than 0) with respect to water content.

After substituting into Eq. (3), we represented heterotrophic respiration as a function of SOC and the environmental drivers:

$$R = k_0 Q_{10}^{(T-15/10)} W^b C \quad (5)$$

Equation (5) was then fit to ESM variables as described below in Sect. 2.4.1 to generate ESM-specific k_0 , Q_{10} , and b parameters.

We also used Eq. (4) to derive the change in decomposition rate by taking the first order derivative as follows:

$$\frac{dk}{dt} = k \left\{ \frac{\ln(Q_{10})}{10} \frac{dT}{dt} + \frac{b}{W} \frac{dW}{dt} \right\} \quad (6)$$

We then assumed that the rate of change can be approximated by a single time step over the entire time period, giving the following simplification:

$$\Delta k = k_{\text{start}} \left\{ \ln(Q_{10}) \frac{\Delta T}{10} + b \frac{\Delta W}{W_{\text{start}}} \right\} \quad (7)$$

where k_{start} , and W_{start} are the contemporary (1997–2006) 10 yr mean of decomposition rate and soil water, respectively; Δk , ΔW , and ΔT are the changes from the contemporary (1997–2006) to the final (2090–2099) 10 yr means of decomposition rate,

BGD

10, 18969–19004, 2013

Soil carbon changes in Earth system models

K. E. O. Todd-Brown et al.

[Title Page](#)

[Abstract](#)

[Introduction](#)

[Conclusions](#)

[References](#)

[Tables](#)

[Figures](#)

[◀](#)

[▶](#)

[◀](#)

[▶](#)

[Back](#)

[Close](#)

[Full Screen / Esc](#)

[Printer-friendly Version](#)

[Interactive Discussion](#)



soil water, and soil temperature. In our analysis we simplified Eq. (7) to include just the temperature term because soil water did not contribute significantly to the model. Gridded values were used for within-model comparisons. Global total SOC and heterotrophic respiration were used for between-model analyses with decomposition rate calculated from the previously mentioned global totals. Area-weighted global mean soil temperature and soil water content were used for the between-model comparisons.

2.4.1 Parameterization

The intrinsic decomposition rate (k_0) and environmental sensitivity parameters (Q_{10} , b) in Eq. (5) were fitted using the ESM initial historical 10 yr gridded mean (1850–1859 in most cases) of heterotrophic respiration, SOC, soil temperature, and soil moisture. The parameters were fitted using a constrained Broyden–Fletcher–Goldfarb–Shanno optimization algorithm, a quasi-Newtonian method, as implemented in R 2.13.1 (R Development Core Team, 2012). This algorithm was selected for parameter fitting because of its robust convergence and short run time. The following variable ranges were considered in the parameterization: $k_0 \in (10^{-4}, 10)$, $Q_{10} \in (1, 4)$, and $b \in (0, 3)$.

3 Results

Over the 21st century, ESMs predicted SOC changes ranging from a 253 PgC gain (HadGEM2-ES) to a 72 PgC loss (MIROC-ESM) with a multi-model mean gain of 63 PgC (Fig. 1, Tables 1 and 2). Five models (HadGEM2-ES, MPI-ESM-MR, BCC-CSM1.1-M, BNU-ESM, and INM-CM4) estimated SOC gains greater than 75 Pg. Four other models (IPSL-CM5A-MR, GFDL-ESM2G, CESM1-BGC, and NorESM1-M) predicted moderate changes in SOC ranging from a 15 PgC gain to a 40 PgC loss. Two models (CanESM2 and MIROC-ESM) projected an SOC loss of more than 50 Pg. In many cases, large absolute changes in SOC also translated into large relative changes,

BGD

10, 18969–19004, 2013

Soil carbon changes in Earth system models

K. E. O. Todd-Brown et al.

[Title Page](#)

[Abstract](#)

[Introduction](#)

[Conclusions](#)

[References](#)

[Tables](#)

[Figures](#)

[◀](#)

[▶](#)

[◀](#)

[▶](#)

[Back](#)

[Close](#)

[Full Screen / Esc](#)

[Printer-friendly Version](#)

[Interactive Discussion](#)



[Title Page](#)[Abstract](#)[Introduction](#)[Conclusions](#)[References](#)[Tables](#)[Figures](#)[◀](#)[▶](#)[◀](#)[▶](#)[Back](#)[Close](#)[Full Screen / Esc](#)[Printer-friendly Version](#)[Interactive Discussion](#)

including a 23 % gain by HadGEM2-ES, a 22 % gain by BCC-CSM1.1-M, and a 14 % gain by BNU-ESM (Fig. 1, Table 2).

For four of the five models with highest gains (more than 75 PgC, HadGEM2-ES, MPI-ESM-MR, BNU-ESM, INM-CM4), most of the global gain was located in boreal and tundra biomes; BCC-CSM1.1-M was an exception, showing roughly equal gains in high and mid-latitude biomes (Table 1). In contrast, the two models showing the greatest losses in SOC (more than 50 PgC, MIROC-ESM and CanESM2) showed most of those losses in the tropical forest and grassland and savanna biomes. Three of the four models with moderate SOC changes showed more SOC change in mid-latitude biomes than in high northern latitude biomes; GFDL-ESM2G was an exception and showed a 37 PgC loss in the northern latitudes balanced by a 41 PgC gain in the mid-latitudes. These diverging patterns were also apparent in maps of SOC change (Fig. 2 and 3) and tended to follow the distribution of SOC at the beginning of the analysis period (Fig. S2).

3.1 Changes in NPP, soil inputs, respiration, and turnover times

All of the models had increases in NPP and thus soil inputs during the 21st century (Table 2, Fig. 1). NPP increases occurred across the globe in most models, with absolute changes ranging from 7 PgCyr⁻¹ (NorESM1-M) to 46 PgCyr⁻¹ (MPI-ESM-MR). Relative global NPP increases varied between 15 % (NorESM1-M) and 59 % (HadGEM2-ES) (Table 2). NPP increases generally followed modern distributions (Figs. S3 and S4); however decreases in NPP were notable in the Amazon basin in three models (BCC-CSM1.1-M, HadGEM2-ES, and CanESM2) and southern sections of North America, southern Africa, and southwest South America in IPSL-CM5A-MR (Figs. S4 and S5). For most models, global SOC inputs for 1997–2006 and 2090–2099 matched the respective mean annual NPP relatively closely, with global differences of less than 7 PgCyr⁻¹ (approximately 15 % of NPP) over the 21st century (Table 2). However there were more substantial differences of 13–36 PgCyr⁻¹ between NPP and soil inputs in three models (IPSL-CM5A-MR, GFDL-ESM2G, MPI-ESM-MR). These

differences could be due to either accumulation of carbon in vegetation (and thus time delays in the delivery of this carbon to SOC pools) or losses through other pathways such as land use change, harvesting, or fire.

Global heterotrophic respiration also increased in all models, with absolute increases ranging from 4 PgCyr^{-1} (NorESM1-M) to 43 PgCyr^{-1} (HadGEM2-ES) (Table 2). These increases in heterotrophic respiration were caused by the increase in soil inputs described above and, simultaneously, decreases in global turnover times between 12 yr (25%; MIROC-ESM) and 2.1 yr (15%; CESM1-BGC) (Fig. 1). In many ESMs, turnover times decreased by 100 yr or more in high northern latitudes (Figs. S6 and S7). For comparison, contemporary heterotrophic respiration fluxes ranged from 43 PgC yr^{-1} (CESM1-BGC and NorESM1-M) to 76 PgCyr^{-1} (MPI-ESM-MR) and turnover times ranged from 13 yr (CESM1-BGC) to 46 yr (MIROC-ESM) (Fig. 1, and starting distributions in Fig. S8).

3.2 Changes in net SOC flux

By the end of the 21st century, the net SOC flux was negative (carbon being lost from the soil), ranging between -0.2 PgCyr^{-1} (BNU-ESM and CESM1-BGC) and -3.0 PgCyr^{-1} (MIROC-ESM) in most models, with the exceptions of HadGEM1-ES ($+2.9 \text{ PgCyr}^{-1}$), BCC-CSM1-M ($+2.1 \text{ PgCyr}^{-1}$), and MPI-ESM-MR ($+1.4 \text{ PgCyr}^{-1}$). Modern net SOC flux had a much smaller range, between -0.5 PgCyr^{-1} (CanESM2) and $+1.9 \text{ PgCyr}^{-1}$ (MIROC-ESM) with a multi-model mean of $+0.6 \text{ PgCyr}^{-1}$. The soils in four models switched from net sinks to net sources of carbon (Table 2).

3.3 Changes in soil temperature and soil moisture

Predicted changes in soil temperature and moisture varied widely across models, with consequences for SOC dynamics. Across all models there was a warming trend over the 21st century in soil temperature (Table 2), with a multi-model mean increase of $4.8 \text{ }^{\circ}\text{C}$ and a range between $3.1 \text{ }^{\circ}\text{C}$ (INM-CM4) and $6.4 \text{ }^{\circ}\text{C}$ (HadGEM1-ES). Warming

BGD

10, 18969–19004, 2013

Soil carbon changes in Earth system models

K. E. O. Todd-Brown et al.

[Title Page](#)

[Abstract](#)

[Introduction](#)

[Conclusions](#)

[References](#)

[Tables](#)

[Figures](#)

[◀](#)

[▶](#)

[◀](#)

[▶](#)

[Back](#)

[Close](#)

[Full Screen / Esc](#)

[Printer-friendly Version](#)

[Interactive Discussion](#)



[Title Page](#)[Abstract](#)[Introduction](#)[Conclusions](#)[References](#)[Tables](#)[Figures](#)[◀](#)[▶](#)[◀](#)[▶](#)[Back](#)[Close](#)[Full Screen / Esc](#)[Printer-friendly Version](#)[Interactive Discussion](#)

was most intense in the high northern latitudes in most models (Fig. S9), ranging between 3.1 °C (INM-CM4, BCC-CSM1.1-M) and 8. °C (MIROC-ESM) when averaged across boreal and arctic tundra biomes (Table S2). In most models, soil temperatures increased in these biomes by a smaller amount than surface air temperatures because
5 loss of snow cover increased winter heat fluxes to the atmosphere.

The change in fractional soil water content over the entire soil column of each model was even more variable across models over the 21st century, with some of the models becoming drier and others becoming wetter (Table 2, Fig. S1) compared to starting distributions shown in Fig. S11. However, the magnitude of change in global mean soil
10 water was relatively small, ranging from –0.046 to 0.007 [kg-water m² kg^{–1} max. water m^{–2}] across the 21st century (Table 2).

3.4 Drivers of SOC change

Changes in global SOC were the net effect of large increases in inputs and decreases in turnover times (Fig. 4). In the constant turnover time scenario (Fig. 4, green lines),
15 between 106 (NorESM1-M) and 1230 (MPI-ESM-MR) PgC of SOC accumulated from 1850 to 2100 across models due to increases in NPP, and thus SOC inputs, over time. Conversely, in the constant carbon input scenario (Fig. 4, red lines), between 104 (MIROC-ESM) and 629 (MPI-ESM-MR) PgC were lost from global soil stocks
20 as soils warmed and heterotrophic respiration increased. For all models, the amount of carbon potentially gained due to increasing inputs over time was greater than the amount carbon potentially lost through increases in decomposition rates. Overall, the magnitude of potential change in SOC input and decomposition was between 2 and over 50 times greater than the predicted change in SOC over the same time period (Fig. 4).

25 Between ESMs, the change in global SOC was well-explained by Eq. (2) using the relative changes in soil inputs and decomposition rates, and the size of the initial SOC ($R^2 = 0.89, p < 0.01$, Fig. 5d). Explanatory power was similarly high when SOC change was expressed as the absolute ($R^2 = 0.88, p < 0.01$, Fig. S12a) or relative ($R^2 = 0.83,$

p < 0.01, Fig. S12b) change in steady state SOC pools, implying that the starting and ending pools are nearly at steady state in the ESMs. The total change in global SOC was not significantly correlated with the initial SOC ($R^2 = 0.01$, $p = 0.81$, Fig. 5a), nor the change decomposition rate ($R^2 = 0.05$, $p = 0.52$, Fig. 5c). Instead, much of this change was attributed to the change in soil inputs ($R^2 = 0.54$, $p < 0.01$, Fig. 5b), with the remaining explanation coming from the interactive effect between initial SOC, changes in soil inputs, and the changes in decomposition rate.

Within most individual ESMs, changes in SOC at each grid cell over the 21st century were well explained by Eq. (2) ($0.87 > R^2 > 0.58$, $p < 0.001$), with the exception of IPSL-CM5A-MR, MIROC-ESM, and MPI-ESM-MR (Table S3). In almost all ESMs, the change in soil inputs explained more variation than the change in decomposition rate, though MIROC-ESM was an exception (Table S3).

3.5 Drivers of change in decomposition between models

Between-model variation in the change of global mean decomposition rate was well explained by model parameterization and environmental variables (Fig. 6). Together, the initial decomposition rate, the temperature sensitivity parameter (Q_{10}) of each ESM, and the ESM-simulated change in soil temperature explained most of the variation between ESMs as modeled by the temperature sensitivity term in Eq. (7) ($R^2 = 0.81$, $p < 0.01$, Fig. 6d). The change in decomposition rate was moderately explained by the initial decomposition rate ($R^2 = 0.44$, $p = 0.03$, Fig. 6a). Other individual terms in Eq. (7), including variation in Q_{10} and ESM-simulated change in soil temperature, did not significantly explain any variation (Fig. 6b and c); nor did the moisture term add any explanatory value.

10, 18969–19004, 2013

BGD

Soil carbon changes in Earth system models

K. E. O. Todd-Brown et al.

[Title Page](#)

[Abstract](#)

[Introduction](#)

[Conclusions](#)

[References](#)

[Tables](#)

[Figures](#)

◀

▶

◀

▶

[Back](#)

[Close](#)

[Full Screen / Esc](#)

[Printer-friendly Version](#)

[Interactive Discussion](#)



4 Discussion

A key determinant of future carbon cycle feedbacks on climate is whether increased inputs from NPP or increased losses due to heterotrophic respiration will dominate SOC responses to global change (Davidson and Janssens, 2006). Much of the recent soil biogeochemical literature has focused on SOC losses through heterotrophic respiration which are expected to increase with global warming (Davidson and Janssens, 2006; Koven et al., 2011); however, previous studies have concluded that the variability in NPP also drives variation in ESM terrestrial carbon storage (Matthews et al., 2005). In our analysis, all of the ESMs predicted that global SOC turnover times will decrease by 15 to 28 % (Fig. 1). However, our analysis shows that most ESMs (seven of eleven) predict increases in global SOC over the 21st century. In these models, increased NPP and SOC inputs from 21st century global change more than offset increases in SOC decomposition.

4.1 SOC decomposition in ESMs

The absolute change in SOC decomposition across ESMs mainly depends on the initial decomposition rate, temperature sensitivity of decomposition, and the temperature change predicted by the models (Fig. 6). Our analysis suggests that these factors vary substantially across ESMs, but the range of variation is broadly consistent with empirical observations. Intrinsic soil organic carbon decomposition rate (fitted at 15 °C and optimal soil moisture) varied between 6 and 24 yr (Table S4), a range consistent with the parameterization of traditional biogeochemical models (e.g. Parton et al., 1993). Q_{10} factors ranged between 1.4 and 2.2 (Table S4) consistent with observed Q_{10} values (Davidson and Janssens, 2006; Fierer et al., 2006; Mahecha et al., 2010). Moisture sensitivity did not provide any additional explanation of variation in decomposition rate changes across ESMs nor did it substantially improve reduced complexity models of heterotrophic respiration within ESMs (Table S4), suggesting that it is not a primary driver of SOC decomposition change in the ESMs considered. However, modeled tem-

[Title Page](#)[Abstract](#)[Introduction](#)[Conclusions](#)[References](#)[Tables](#)[Figures](#)[◀](#)[▶](#)[Back](#)[Close](#)[Full Screen / Esc](#)[Printer-friendly Version](#)[Interactive Discussion](#)

perature and moisture changes in the ESMs remain a key source of uncertainty that will only be resolved as models are tested against observations of future global change (Knutti and Sedláček, 2012).

4.2 NPP and SOC inputs in ESMs

5 All ESMs predicted substantial (15–59 %) increases in NPP over the 21st century (Table 2). These increases are primarily due to CO₂ fertilization effects, and secondarily due to temperature and moisture change (Anav et al., 2013). Although plausible based on FACE studies (Norby et al., 2010; Piao et al., 2013), the increases in SOC inputs predicted by ESMs should be considered an upper bound for the 21st century. Several factors could reduce the predicted positive impact of rising CO₂ concentrations on 10 SOC storage. First, FACE studies have only been conducted in a limited number of ecosystems that are not representative of the entire terrestrial biosphere. FACE studies tend to be located in ecosystems with relatively high CO₂ sensitivity, such as early- to mid-successional systems with high nutrient supply and rapidly growing vegetation 15 (Körner, 2006; Norby and Zak, 2011). Ecosystems with closed nutrient cycles and full canopy development occupy the largest fraction of the global land surface and current studies show a more limited CO₂ fertilization response in these ecosystems (Bader et al., 2013).

Some of these constraints could be alleviated by other aspects of global change, 20 for example increased nutrient mineralization under soil warming or increased nutrient inputs from atmospheric deposition (Bai et al., 2013; Rustad et al., 2001). However, some constraints could also be exacerbated; for instance reduced precipitation or increased evapotranspiration under climate change could lead to increased water limitation of NPP. Similarly, N and P could become progressively more limiting as biomass 25 increases (Exbrayat et al., 2013). Nutrients could be further limited by increases in precipitation potentially leading to increased nutrient runoff.

Even if the terrestrial biosphere does respond to elevated CO₂ in line with FACE studies, it is unclear how long this response can be maintained. In ESMs, the majority

BGD

10, 18969–19004, 2013

Soil carbon changes in Earth system models

K. E. O. Todd-Brown et al.

Title Page	
Abstract	Introduction
Conclusions	References
Tables	Figures
◀	▶
◀	▶
Back	Close
Full Screen / Esc	
Printer-friendly Version	
Interactive Discussion	



of predicted change in NPP and SOC inputs occurs beyond 550 ppm CO₂, a range unexplored in ecosystem studies. Additionally, FACE studies examine an instantaneous change in CO₂, not the relatively gradual CO₂ change simulated in ESMs. The constant turnover time scenarios in Fig. 4 suggest that NPP sensitivity to global change (including CO₂ change) is sustained throughout the 21st century in ESMs, well beyond the conditions simulated by most field experiments. Although a sustained response cannot be ruled out based on current experimental evidence, many photosynthetic processes saturate at high CO₂ concentrations (Franks et al., 2013; Körner, 2006). If NPP were to increase by nearly 50 % over the 21st century, as predicted by some ESMs, negative feedbacks on NPP would be expected at the ecosystem scale as previously discussed.

In addition to potentially overestimating the 21st century NPP response, ESMs likely overestimate the increase of SOC pools in response to this increased input. We found a strong relationship between the change in carbon inputs to soil and SOC change in ESMs (Fig. 5b). Even stronger relationships have been established between the spatial pattern of contemporary NPP and SOC in ESMs (Todd-Brown et al., 2013). However, there is empirical and theoretical evidence that increases in soil inputs, especially under elevated CO₂, may have little effect on SOC stocks (Bader et al., 2013; Norby and Zak, 2011). CO₂ fertilization often increases the labile fractions of plant litter and root exudation (Phillips et al., 2011; Schlesinger and Lichter, 2001). These inputs enter fast turnover carbon pools and are hypothesized to facilitate the decomposition of slow turnover pools through priming (Neill and Gignoux, 2006). All of these ESMs contain first order linear decomposition models of SOC and are thus unable to represent priming mechanisms (Wutzler and Reichstein, 2008). In addition, the availability of mineral surfaces (Six et al., 2002) may constrain the amount of SOC that can be stored in a given soil. These effects will likely weaken the coupling between NPP and SOC changes.

Finally, land use change can significantly affect NPP and land carbon storage. In one recent analysis with a subset of CMIP5 models, land use change resulted in terrestrial carbon losses of 25 to 205 Pg C compared with no land use change (Brovkin et al.,

BGD

10, 18969–19004, 2013

Soil carbon changes in Earth system models

K. E. O. Todd-Brown et al.

[Title Page](#)

[Abstract](#)

[Introduction](#)

[Conclusions](#)

[References](#)

[Tables](#)

[Figures](#)

◀

▶

◀

▶

[Back](#)

[Close](#)

[Full Screen / Esc](#)

[Printer-friendly Version](#)

[Interactive Discussion](#)



2013). This change is on the same order of magnitude as the 21st century change in soil carbon simulated by many ESMs. Therefore land use change is a critical component of the terrestrial carbon cycle and is likely the driver of some of the variation in SOC not explained by parameterization and environmental variables in our analysis.

5 4.3 Assessing reliability of SOC predictions

One possible approach for narrowing the likely range of SOC predictions is to select estimates of SOC change from ESMs that are consistent with global benchmark datasets (Fig. 7). We compared ESMs outputs to modern SOC stocks and NPP. Two models fell within empirical estimates (BCC-CSM-1.1M and CanESM2), and two additional models matched one empirical estimate and were close to the second (HadGEM-ES and INM-CM4). All other models widely missed at least one benchmark. Models consistent with the benchmarks did not have a markedly narrower range of simulated change in SOC; CanESM2 showed losses of 51 PgC, and BCC-CSM1.1M showed gains of 203 PgC. This wide range suggests that contemporary NPP and SOC benchmarks are not strong constraints on ESM simulations of future soil carbon change.

The spatial pattern of SOC change provides another criterion for evaluating the likelihood of ESM predictions. All ESMs that predicted large SOC gains globally (i.e. greater than 75 PgC) also showed large gains in tundra and boreal biomes (greater than 46 PgC; Table 1). These models include BCC-CSM1.1-M and INM-CM4, which were among the three models most consistent with benchmarking data. In contrast to these model predictions, empirical studies suggest that high-latitude soils are unlikely to serve as a long-term carbon sink (Schuur et al., 2009; Sistla et al., 2013). Even if tundra and boreal NPP were to increase substantially, SOC storage will likely be constrained by permafrost melting, increases in fire frequency and severity, and high vulnerability of old SOC to decomposition under global change (Flannigan et al., 2009; Kasischke and Turetsky, 2006; Mack et al., 2004; Turetsky et al., 2011). Thus all of the ESMs predicting large gains in global SOC appear to depend on unrealistic levels of carbon storage in the high latitudes. This bias likely arises from the lack of permafrost

BGD

10, 18969–19004, 2013

Soil carbon changes in Earth system models

K. E. O. Todd-Brown et al.

[Title Page](#)

[Abstract](#)

[Introduction](#)

[Conclusions](#)

[References](#)

[Tables](#)

[Figures](#)

◀

▶

◀

▶

[Back](#)

[Close](#)

[Full Screen / Esc](#)

[Printer-friendly Version](#)

[Interactive Discussion](#)



5 dynamics in many current ESMs. Although some ESMs represent freeze-thaw dynamics, it is not clear that this representation captures permafrost dynamics that include highly localized changes in hydrological conditions. ESMs that do not predict SOC accumulation in the high latitudes tend to predict SOC losses or much smaller gains at the global scale.

5 Conclusions

Our work shows that most current ESMs project sustained or increasing carbon sequestration potential in global soils over the 21st century. Although decomposition rates increase with climate warming, this effect is largely offset by CO₂-driven increases in 10 NPP and soil inputs. Unrecognized constraints on future NPP response or limits on the conversion of plant inputs to SOC could therefore substantially reduce soil carbon storage. In particular, constraints on NPP are uncertain because ecosystem-scale CO₂ manipulations have not been carried out above 550 ppm, a value that may be exceeded by mid-century. As a result, our analysis questions the current majority of 15 ESMs that show a sustained SOC sink in the face of 21st century global change. Although a few ESMs are consistent with modern benchmark datasets, we conclude that there is a considerable downside risk to future terrestrial carbon storage in soils from processes that are not currently represented within current ESMs.

New modeling efforts should consider quantifying constraints on the NPP response 20 to global change and altering SOC sub-models to represent mechanisms responsible for SOC response to NPP change. For example, incorporating nutrient dynamics into ESMs could help constrain the NPP response to CO₂ fertilization (Exbrayat et al., 2013; Piao et al., 2013; Thornton et al., 2009), and all model structures could be updated to account for microbial priming effects (Wieder et al., 2013) and mineral-SOC interactions 25 (Six et al., 2000; Torn et al., 1997). Biogeochemical responses in ESMs should continue to be tested for congruence with global datasets (e.g. Todd-Brown et al., 2013), age distributions derived from radiocarbon observations (Trumbore, 2009), and well-known

BGD

10, 18969–19004, 2013

Soil carbon changes in Earth system models

K. E. O. Todd-Brown et al.

[Title Page](#)

[Abstract](#)

[Introduction](#)

[Conclusions](#)

[References](#)

[Tables](#)

[Figures](#)

◀

▶

◀

▶

[Back](#)

[Close](#)

[Full Screen / Esc](#)

[Printer-friendly Version](#)

[Interactive Discussion](#)



empirical results from global change experiments across diverse ecosystems (Norby and Zak, 2011; Rustad et al., 2001). These efforts will help ensure that policy makers can develop mitigation strategies for global change based on accurate projections of the global carbon cycle.

5 **Supplementary material related to this article is available online at
[http://www.biogeosciences-discuss.net/10/18969/2013/
bgd-10-18969-2013-supplement.pdf](http://www.biogeosciences-discuss.net/10/18969/2013/bgd-10-18969-2013-supplement.pdf).**

10 *Acknowledgements.* We would like to thank the National Science Foundation (Advancing Theory in Biology and Decadal and Regional Climate Prediction using Earth System Models (EaSM) programs) and the Department of Energy Office of Science Biological and Environmental Research (BER) for funding this research. We also acknowledge the World Climate Research Programme's Working Group on Coupled Modeling, which is responsible for CMIP, and we thank the model groups (listed in Table S1 of this paper) for producing and making available their model output. We thank the US Department of Energy's Program for Climate model Diagnosis and Intercomparison for providing coordinating support and leading development of software infrastructure in partnership with Global Organization for Earth System Science Portals. We would also like to thank Christian Reick for his contribution of the MPI-ESM simulations and manuscript review.

15

References

20 Anav, A., Friedlingstein, P., Kidston, M., Bopp, L., Caias, P., Cox, P., Jones, C., Jung, M., My-
neni, R., and Zhu, Z.: Evaluating the land and ocean components of the global carbon cy-
cle in the CMIP5 Earth system models, *J. Climate*, 26, 6801–6843, doi:10.1175/JCLI-D-12-
00417.1, 2013.

25 Bader, M. K.-F., Leuzinger, S., Keel, S. G., Siegwolf, R. T. W., Hagedorn, F., Schleppi, P.,
and Körner, C.: Central European hardwood trees in a high- CO_2 future: synthesis of an

BGD

10, 18969–19004, 2013

Soil carbon changes in Earth system models

K. E. O. Todd-Brown et al.

Title Page	
Abstract	Introduction
Conclusions	References
Tables	Figures
◀	▶
◀	▶
Back	Close
Full Screen / Esc	
Printer-friendly Version	
Interactive Discussion	



Soil carbon changes in Earth system models

K. E. O. Todd-Brown et al.

[Title Page](#)

[Abstract](#)

[Introduction](#)

[Conclusions](#)

[References](#)

[Tables](#)

[Figures](#)

◀

▶

◀

▶

[Back](#)

[Close](#)

[Full Screen / Esc](#)

[Printer-friendly Version](#)

[Interactive Discussion](#)



Soil carbon changes in Earth system models

K. E. O. Todd-Brown et al.

[Title Page](#)

[Abstract](#)

[Introduction](#)

[Conclusions](#)

[References](#)

[Tables](#)

[Figures](#)

◀

▶

◀

▶

[Back](#)

[Close](#)

[Full Screen / Esc](#)

[Printer-friendly Version](#)

[Interactive Discussion](#)



Title Page

Abstract

Introduction

Conclusions

References

Tables

Figures

|◀

▶|

◀

▶|

Back

Close

Full Screen / Esc

Printer-friendly Version

Interactive Discussion



Koven, C. D., Ringeval, B., Friedlingstein, P., Ciais, P., Cadule, P., Khvorostyanov, D., Krinner, G., and Tarnocai, C.: Permafrost carbon–climate feedbacks accelerate global warming, *P. Natl. Acad. Sci. USA*, 108, 14769–14774, doi:10.1073/pnas.1103910108, 2011.

Kuzyakov, Y., Friedel, J. K., and Stahr, K.: Review of mechanisms and quantification of priming effects, *Soil Biol. Biochem.*, 32, 1485–1498, doi:10.1016/S0038-0717(00)00084-5, 2000.

Lloyd, J. and Taylor, J. A.: On the temperature dependence of soil respiration, *Funct. Ecol.*, 8, 315–323, 1994.

Luo, Y., Su, B., Currie, W. S., Dukes, J. S., Finzi, A., Hartwig, U., Hungate, B., Mc Murtrie, R. E., Oren, R., Parton, W. J., Pataki, D. E., Shaw, M. R., Zak, D. R., and Field, C. B.: Progressive nitrogen limitation of ecosystem responses to rising atmospheric carbon dioxide, *Bioscience*, 54, 731, doi:10.1641/0006-3568(2004)054[0731:PNLOER]2.0.CO;2, 2004.

Mack, M. C., Schuur, E. A. G., Bret-Harte, M. S., Shaver, G. R., and Chapin, F. S.: Ecosystem carbon storage in arctic tundra reduced by long-term nutrient fertilization, *Nature*, 431, 440–443, 2004.

Mahecha, M. D., Reichstein, M., Carvalhais, N., Lasslop, G., Lange, H., Seneviratne, S. I., Vargas, R., Ammann, C., Arain, M. A., Cescatti, A., Janssens, I. A., Migliavacca, M., Montagnani, L., and Richardson, A. D.: Global convergence in the temperature sensitivity of respiration at ecosystem level, *Science*, 329, 838–840, doi:10.1126/science.1189587, 2010.

Matthews, H. D., Eby, M., Weaver, A. J., and Hawkins, B. J.: Primary productivity control of simulated carbon cycle-climate feedbacks, *Geophys. Res. Lett.*, 32, L14708, doi:10.1029/2005GL022941, 2005.

NASA Land Processes Distributed Active Archive Center (LP DAAC): Land Cover Type Yearly L3 Global 0.05Deg CMG (MCD12C1), USGS/Earth Resour. Obs. Sci. Center, Sioux Falls, South Dakota, available at: https://lpdaac.usgs.gov/products/modis_products_table/mcd12c1, 2008.

Neill, C. and Gignoux, J.: Soil organic matter decomposition driven by microbial growth: A simple model for a complex network of interactions, *Soil Biol. Biochem.*, 38, 803–811, doi:10.1016/j.soilbio.2005.07.007, 2006.

Norby, R. J. and Zak, D. R.: Ecological lessons from free-air CO₂ enrichment (FACE) experiments, *Annu. Rev. Ecol. Evol. S.*, 42, 181–203, doi:10.1146/annurev-ecolsys-102209-144647, 2011.

Norby, R. J., DeLucia, E. H., Gielen, B., Calfapietra, C., Giardina, C. P., King, J. S., Ledford, J., McCarthy, H. R., Moore, D. J. P., Ceulemans, R., De Angelis, P., Finzi, A. C., Karnosky,

D. F., Kubiske, M. E., Lukac, M., Pregitzer, K. S., Scarascia-Mugnozza, G. E., Schlesinger, W. H., and Oren, R.: Forest response to elevated CO₂ is conserved across a broad range of productivity, *P. Natl. Acad. Sci. USA*, 102, 18052–18056, doi:10.1073/pnas.0509478102, 2005.

5 Norby, R. J., Warren, J. M., Iversen, C. M., Medlyn, B. E., and McMurtrie, R. E.: CO₂ enhancement of forest productivity constrained by limited nitrogen availability, *P. Natl. Acad. Sci. USA*, 107, 19368–19373, doi:10.1073/pnas.1006463107, 2010.

10 Nowak, R. S., Ellsworth, D. S., and Smith, S. D.: Functional responses of plants to elevated atmospheric CO₂ – do photosynthetic and productivity data from FACE experiments support early predictions?, *New Phytol.*, 162, 253–280, doi:10.1111/j.1469-8137.2004.01033.x, 2004.

15 Pan, Y., Birdsey, R. A., Fang, J., Houghton, R., Kauppi, P. E., Kurz, W. A., Phillips, O. L., Shvidenko, A., Lewis, S. L., Canadell, J. G., Ciais, P., Jackson, R. B., Pacala, S. W., McGuire, A. D., Piao, S., Rautiainen, A., Sitch, S., and Hayes, D.: A large and persistent carbon sink in the world's forests, *Science*, 333, 988–993, doi:10.1126/science.1201609, 2011.

20 Parton, W. J., Scurlock, J. M. O., Ojima, D. S., Gilmanov, T. G., Scholes, R. J., Schimel, D. S., Kirchner, T., Menaut, J., Seastedt, T., Garcia Moya, E., Kamnalrut, A., and Kinyamario, J. I.: Observations and modeling of biomass and soil organic matter dynamics for the grassland biome worldwide, *Global Biogeochem. Cy.*, 7, 785–809, doi:10.1029/93GB02042, 1993.

25 Phillips, R. P., Finzi, A. C., and Bernhardt, E. S.: Enhanced root exudation induces microbial feedbacks to N cycling in a pine forest under long-term CO₂ fumigation, *Ecol. Lett.*, 14, 187–194, doi:10.1111/j.1461-0248.2010.01570.x, 2011.

30 Piao, S., Sitch, S., Ciais, P., Friedlingstein, P., Peylin, P., Wang, X., Ahlström, A., Anav, A., Canadell, J. G., Cong, N., Huntingford, C., Jung, M., Levis, S., Levy, P. E., Li, J., Lin, X., Lomas, M. R., Lu, M., Luo, Y., Ma, Y., Myneni, R. B., Poulter, B., Sun, Z., Wang, T., Viovy, N., Zaehle, S., and Zeng, N.: Evaluation of terrestrial carbon cycle models for their response to climate variability and to CO₂ trends, *Glob. Change Biol.*, 19, 2117–2132, doi:10.1111/gcb.12187, 2013.

Le Quéré, C., Raupach, M. R., Canadell, J. G., Marland, G., Bopp, L., Ciais, P., Conway, T. J., Doney, S. C., Feely, R. A., Foster, P., Friedlingstein, P., Gurney, K., Houghton, R. A., House, J. I., Huntingford, C., Levy, P. E., Lomas, M. R., Majkut, J., Metzl, N., Ometto, J. P., Peters, G. P., Prentice, I. C., Randerson, J. T., Running, S. W., Sarmiento, J. L., S. U., Sitch, S.,

**Soil carbon changes
in Earth system
models**[Title Page](#)[Abstract](#)[Introduction](#)[Conclusions](#)[References](#)[Tables](#)[Figures](#)[|◀](#)[▶|](#)[◀](#)[▶](#)[Back](#)[Close](#)[Full Screen / Esc](#)[Printer-friendly Version](#)[Interactive Discussion](#)

Soil carbon changes in Earth system models

K. E. O. Todd-Brown et al.

[Title Page](#)

[Abstract](#)

[Introduction](#)

[Conclusions](#)

[References](#)

[Tables](#)

[Figures](#)

[◀](#)

[▶](#)

[◀](#)

[▶](#)

[Back](#)

[Close](#)

[Full Screen / Esc](#)

[Printer-friendly Version](#)

[Interactive Discussion](#)



CMIP5 Earth system models and comparison with observations, *Biogeosciences*, 10, 1717–1736, doi:10.5194/bg-10-1717-2013, 2013.

Torn, M. S., Trumbore, S. E., Chadwick, O. A., Vitousek, P. M., and Hendricks, D. M.: Mineral control of soil organic carbon storage and turnover, *Nature*, 389, 170–173, 1997.

5 Trumbore, S.: Radiocarbon and soil carbon dynamics, *Annu. Rev. Earth Planet. Sci.*, 37, 47–66, doi:10.1146/annurev.earth.36.031207.124300, 2009.

Turetsky, M. R., Kane, E. S., Harden, J. W., Ottmar, R. D., Manies, K. L., Hoy, E., and Kasischke, E. S.: Recent acceleration of biomass burning and carbon losses in Alaskan forests and peatlands, *Nat. Geosci.*, 4, 27–31, 2011.

10 Wieder, W. R., Bonan, G. B., and Allison, S. D.: Global soil carbon projections are improved by modelling microbial processes, *Nat. Clim. Chang.*, 3, 909–912, 2013.

Wutzler, T. and Reichstein, M.: Colimitation of decomposition by substrate and decomposers – a comparison of model formulations, *Biogeosciences*, 5, 749–759, doi:10.5194/bg-5-749-2008, 2008.

BGD

10, 18969–19004, 2013

Soil carbon changes in Earth system models

K. E. O. Todd-Brown et al.

[Title Page](#)

[Abstract](#)

[Introduction](#)

[Conclusions](#)

[References](#)

[Tables](#)

[Figures](#)

◀

▶

◀

▶

[Back](#)

[Close](#)

[Full Screen / Esc](#)

[Printer-friendly Version](#)

[Interactive Discussion](#)



	CESM1-BGC	NorESM1-M	BNU-ESM	BCC-CSM1.1-M	HadGEM2-ES	IPSL-CM5A-MR	GFDL-ESM2G	CanESM2	INM-CM4	MIROC-ESM	MPI-ESM-MR	Multi-model mean
Tundra	3	-1	54	50	85	2	-9	3	24	1	64	25
Boreal forest	-1	-5	18	47	61	-5	-28	-6	22	-22	62	13
Tropical rainforest	-11	-17	4	14	5	14	6	-15	9	-34	9	-1
Temperate forest	-2	-5	0	7	11	0	2	-1	0	-5	6	1
Desert and shrubland	2	0	11	16	16	2	13	-3	4	14	69	13
Grasslands and savanna	1	-7	8	37	36	3	7	-20	10	3	-10	6
Cropland and urban	4	-6	2	32	34	-2	13	-9	6	-31	7	4
Permanent wetlands	0	0	0	0	2	0	-2	0	0	-2	3	0
Snow and ice	0	0	2	0	3	0	0	0	0	4	1	1
Northern latitude	2	-5	72	97	146	-2	-37	-3	46	-21	126	38
Mid-latitude	-6	-35	25	106	102	18	41	-48	29	-53	81	24
Total	-4	-40	99	203	253	15	1	-51	76	-72	211	63

Title Page

Abstract

Introduction

Conclusions

References

Tables

Figures

◀

▶

◀

▶

Back

Close

Full Screen / Esc

Printer-friendly Version

Interactive Discussion

Table 2. Starting values (1997–2006 mean), final value (2090–2099 mean), absolute change, and relative change of soil carbon, net primary productivity (NPP), soil inputs, heterotrophic respiration, net SOC flux (positive values are carbon gains by the SOC pool, negative values are carbon losses), soil temperature, and normalized soil water content. Normalized soil water content is mean gridded soil water content divided by the grid maximum soil water content at the 10 yr initial historical mean value.

		CESM1-BGC	NorESM1-M	BNU-ESM	BCC-CSM1-1M	HadGEM2-ES	IPSL-CM5A-MR	GFDL-ESM2G	CanESM2	INM-CM4	MIROC-ESM	MPI-ESM-MR	Multi-model mean
SOC [Pg C]	2006	575	610	704	930	1121	1396	1411	1539	1683	2565	3101	1421
	2099	571	570	803	1134	1374	1412	1412	1488	1759	2493	3312	1484
	Abs. Change	-4	-40	99	203	253	15	1	-51	76	-72	211	63
	Rel. Change (%)	-0.6	-7.0	14.0	21.9	22.6	1.1	0.1	-3.3	4.5	-2.8	6.8	5.2
NPP [PgCyr ⁻¹]	2006	46	47	50	58	75	84	78	65	68	63	93	66
	2099	56	54	72	85	120	116	118	86	85	78	138	92
	Abs. Change	10	7	22	27	45	31	40	21	17	15	46	25
	Rel. Change (%)	22.1	14.8	43.8	46.9	59.3	37.0	50.4	32.4	25.1	23.7	49.1	36.8
SOC inputs [PgCyr ⁻¹]	2006	43	43	49	57	75	69	65	65	67	57	77	61
	2099	50	47	70	87	119	92	91	84	83	70	102	81
	Abs. Change	7	4	21	29	44	23	26	20	16	13	25	21
	Rel. Change (%)	17.0	8.2	44.0	51.6	59.3	32.8	39.8	30.3	24.7	22.8	32.4	33.0
Heterotrophic respiration [PgCyr ⁻¹]	2006	43	43	48	56	73	69	66	65	66	55	76	60
	2099	50	48	70	85	116	93	92	85	83	73	101	81
	Abs. Change	7	4	22	28	43	24	26	20	18	18	25	21
	Rel. Change (%)	17.5	10.1	46.8	50.5	58.3	34.3	40.0	30.4	27.1	32.5	33.1	34.6
Net SOC flux [PgCyr ⁻¹]	2006	0.0	0.0	0.8	0.9	1.4	0.5	-0.4	-0.5	1.0	1.9	1.5	0.6
	2099	-0.2	-0.8	-0.2	2.1	3.0	-0.4	-0.6	-0.7	-0.4	-3.0	1.4	0.0
	Abs. Change	-0.2	-0.8	-1.0	1.2	1.6	-0.9	-0.3	-0.2	-1.3	-4.9	-0.1	-0.6
Soil temperature [°C]	2006	16.4	14.5	17.2	17.2	14.8	14.2	14.0	15.7	11.1	16.4	14.6	15.1
	2099	20.2	18.6	21.5	20.9	21.3	20.3	17.8	21.8	14.2	22.6	19.7	19.9
	Abs. Change	3.8	4.1	4.3	3.8	6.4	6.1	3.8	6.1	3.1	6.2	5.1	4.8
Soil water [kg m ⁻² water kg ⁻¹ m ⁻² max. water]	2006	0.249	0.036	0.261	0.189	0.498	0.675	0.560	0.119	0.354	0.651	0.311	0.355
	2099	0.253	0.036	0.263	0.195	0.468	0.629	0.553	0.121	0.353	0.651	0.310	0.349
Abs. Change		0.004	0.000	0.002	0.007	-0.030	-0.046	-0.007	0.002	-0.001	0.001	-0.001	-0.006

Soil carbon changes in Earth system models

K. E. O. Todd-Brown et al.

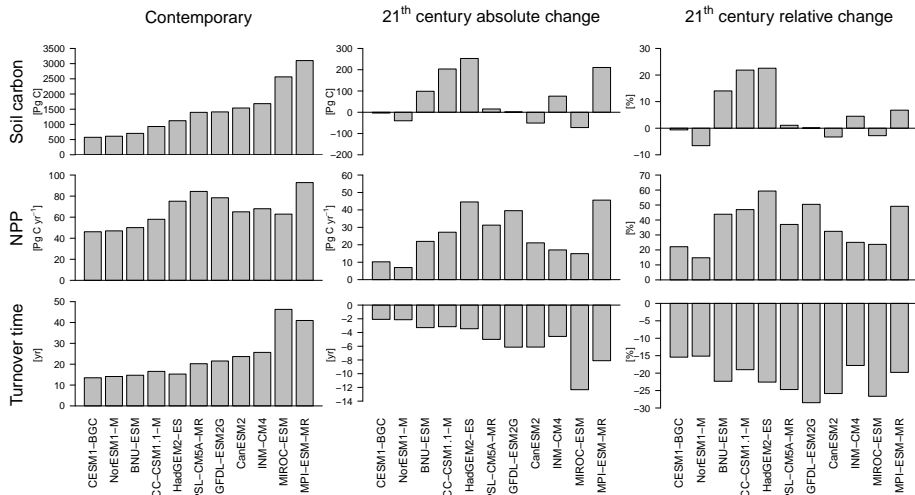


Fig. 1. Contemporary values, absolute changes, and relative changes of soil carbon, net primary production (NPP), and turnover times for CMIP5 Earth system models. Contemporary values of soil carbon, NPP, and turnover times are reported for the 1997–2006 mean using model output from the historical experiment. Changes for the 21st century were estimated from the difference between 2090–2099 and 1997–2006 mean model estimates from the RCP 8.5 experiment. Turnover times were calculated from global soil carbon stocks divided by global heterotrophic respiration.

- [Title Page](#)
- [Abstract](#) [Introduction](#)
- [Conclusions](#) [References](#)
- [Tables](#) [Figures](#)
- [◀](#) [▶](#)
- [◀](#) [▶](#)
- [Back](#) [Close](#)
- [Full Screen / Esc](#)
- [Printer-friendly Version](#)
- [Interactive Discussion](#)

Soil carbon changes in Earth system models

K. E. O. Todd-Brown et al.

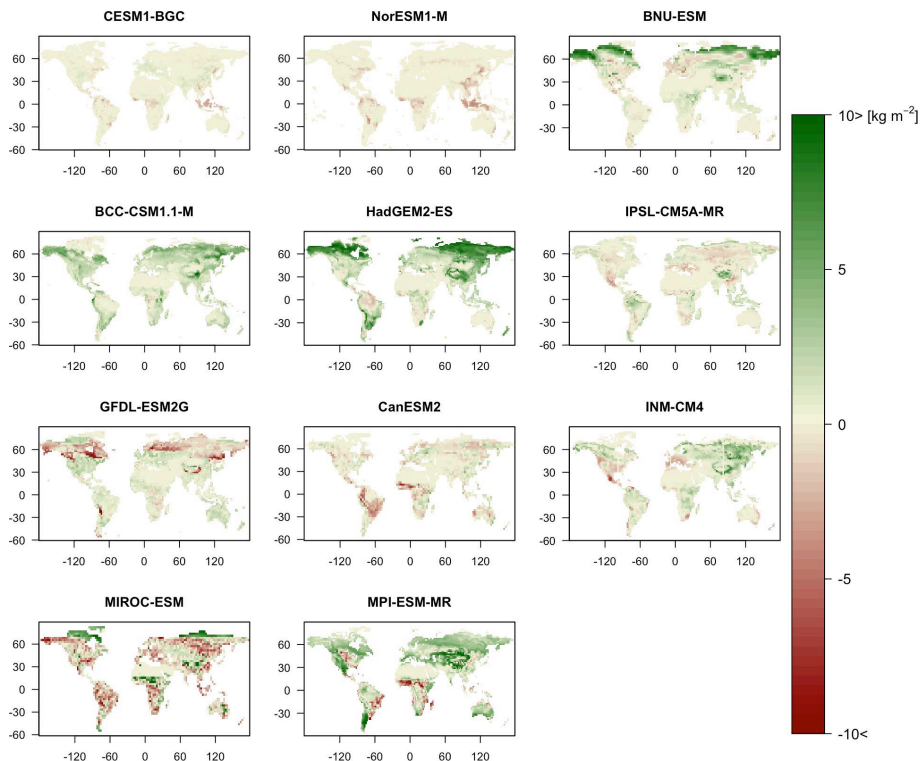


Fig. 2. Absolute change in soil carbon density [kg m^{-2}] over the 21st century for all models (difference in 10 yr means; 2090–2099 minus 1997–2006).

Soil carbon changes in Earth system models

K. E. O. Todd-Brown et al.

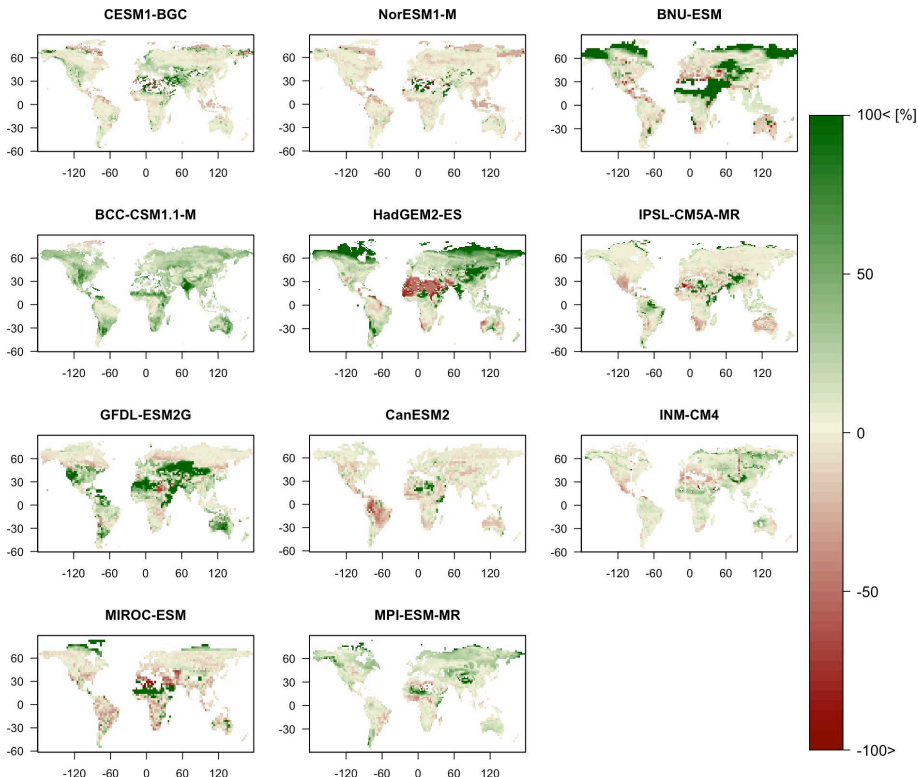


Fig. 3. Relative change in soil carbon density [%] over the 21st century for all models (difference in 10 yr means divided by modern soil carbon density; 2090–2099 minus 1997–2006 divided by 1997–2006).

Soil carbon changes in Earth system models

K. E. O. Todd-Brown et al.

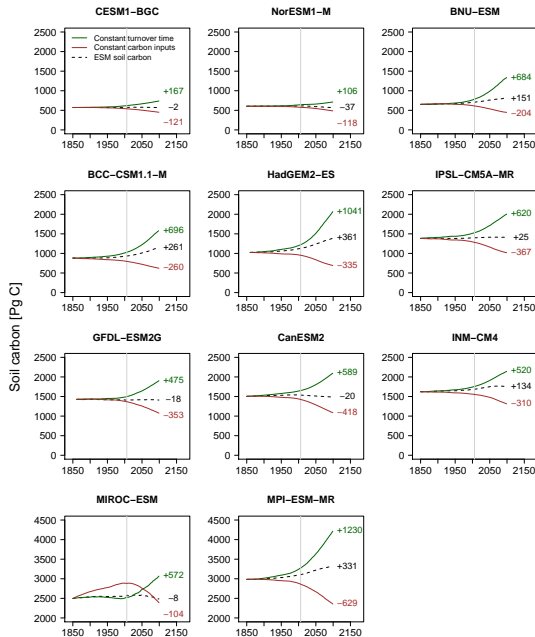


Fig. 4. Soil carbon over time (historical and RCP 8.5) under the “Constant turnover time” and “Constant carbon inputs” scenarios. The black dashed line is the ESM-simulated global soil carbon stock with the net change from 1850 indicated in black text. The green line is the soil carbon stock that would be predicted if turnover time were held constant at the 1850 value and soil inputs were allowed to evolve as predicted by the ESM, with the net change indicated in green text. The red line is the soil carbon stock that would be predicted if carbon inputs were held constant at 1850 levels and the turnover time were allowed to evolve as predicted by the ESM, with the net change in red text. The vertical grey line at 2006 indicates where the historical experiment ends and the RCP 8.5 experiment begins.

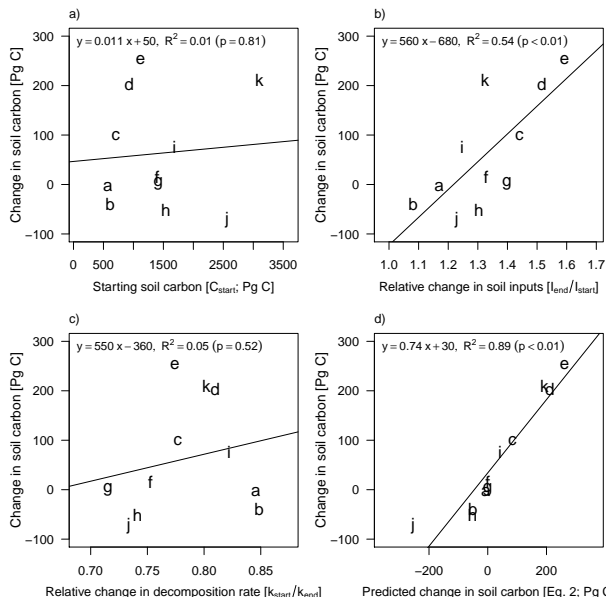


Fig. 5. Change in global soil organic carbon between 1997–2006 and 2090–2099 global means as a function of **(a)** starting soil carbon stock, C_{start} , **(b)** relative change in soil inputs (l), $\frac{l_{\text{end}}}{l_{\text{start}}}$, **(c)** the inverse of the relative change in decomposition rate (k), $\frac{k_{\text{start}}}{k_{\text{end}}}$, and **(d)** Eq. (2), the relative change in steady state times the initial soil carbon stock, $\left(\frac{l_{\text{end}} \times k_{\text{start}}}{k_{\text{end}} \times l_{\text{start}}} - 1\right) \times C_{\text{start}}$. The models are represented as follows; a: CESM1-BGC, b: NorESM1-M, c: BNU-ESM, d: BCC-CSM1.1-M, e: HadGEM2-ES, f: IPSL-CM5A-MR, g: GFDL-ESM2G, h: CanESM2, i: INM-CM4, j: MIROC-ESM, and k: MPI-ESM-MR.

- [Title Page](#)
- [Abstract](#) [Introduction](#)
- [Conclusions](#) [References](#)
- [Tables](#) [Figures](#)
- [◀](#) [▶](#)
- [◀](#) [▶](#)
- [Back](#) [Close](#)
- [Full Screen / Esc](#)
- [Printer-friendly Version](#)
- [Interactive Discussion](#)

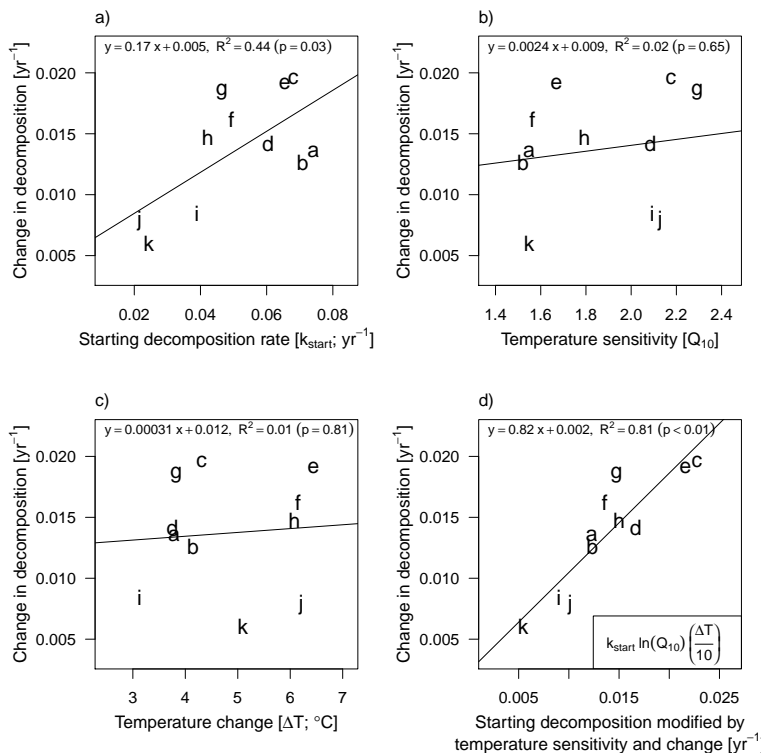


Fig. 6. Change in decomposition rate between 1997–2006 and 2009–2099 global means due to variation in **(a)** starting decomposition rate, k_{start} , **(b)** change in soil temperature, ΔT , **(c)** temperature sensitivity, Q_{10} , and **(d)** starting decomposition rate, Q_{10} , and soil temperature change from Eq. (7), $k_{\text{start}} \ln(Q_{10}) \left(\frac{\Delta T}{10} \right)$. The models are represented as follows; a: CESM1-BGC, b: NorESM1-M, c: BNU-ESM, d: BCC-CSM1.1-M, e: HadGEM2-ES, f: IPSL-CM5A-MR, g: GFDL-ESM2G, h: CanESM2, i: INM-CM4, j: MIROC-ESM, and k: MPI-ESM-MR.

	Abs. ΔC_{soil} [Pg C]	NPP [Pg C yr $^{-1}$]	C_{soil} [Pg C]
CESM1-BGC	-4	46	575
NorESM1-M	-40	47	610
BNU-ESM	99	50	704
BCC-CSM1.1	203	58	930
HadGEM2-ES	253	75	1121
IPSL-CM5A-MR	15	84	1396
GFDL-ESM2G	1	78	1411
CanESM2	-51	65	1539
INM-CM4	76	68	1683
MIROC-ESM	-72	63	2565
MPI-ESM-MR	211	93	3101
Benchmark range		46-73	890-1660

Fig. 7. Metrics of ESM performance and benchmarks for soil C change, net primary production (NPP), and modern soil carbon pools. Benchmark data are shown in the bottom row. Blue cells indicate ESM outputs that fall below the benchmarks, yellow cells are consistent with benchmarks, and red cells are above the benchmarks. NPP data are from Ito (2011); modern soil carbon stocks are from Todd-Brown et al. (2013) and originally from (FAO/IIASA/ISRIC/ISSCAS/JRC, 2012).



Title Page

Abstract

Introduction

Conclusions

References

Tables

Figures

|◀

▶|

◀

▶

Back

Close

Full Screen / Esc

Printer-friendly Version

Interactive Discussion